Water Supply

Water Supply Vol 22 No 4, 4361 doi: 10.2166/ws.2022.055

Numerical investigation of the flow-field characteristics around the suspended pipeline under oblique flows

Qinghua Yang [a], Qian Yang [a,b,*] and Yuqian Zhang [c]

[a] School of Civil Engineering, Southwest Jiaotong University, Chengdu 610031, China
[b] China MCC5 Group Corp. Ltd., Chengdu 610063, China
[c] Pengzhou Water Authority, Chengdu 611930, China
*Corresponding author. E-mail: yangqian-swjtu@foxmail.com

QY, 0000-0002-3293-6052; QY, 0000-0003-4842-2395

ABSTRACT

The flow field distribution around the suspended pipeline is closely related to the mechanical characteristics and local scour characteristics of the underwater crossing pipelines. To fully investigate the velocity distribution and wake structure characteristics around the suspended pipeline under oblique flows, a flume model test and a numerical simulation based on the LES (Large Eddy Simulation) method were performed. The results showed that the velocity distribution near the suspended pipeline under oblique flows had obvious three-dimensional characteristics. The influence range of pipeline on velocity is 1 d before to 6 d behind the pipeline (d is pipeline diameter). The smaller the flow angle, the more disordered the velocity distribution is. The larger the flow angle, the greater the variation degree of the velocity at each section at the same section is, as well as the higher the velocity deficit value is. In addition, the larger the angle of pipe flow, the more violent the wake structure changes with the flow velocity, and the stronger the regularity of vortex street shedding. This research provides a theoretical reference for the scour prevention design and safe operation of crossing pipelines.

Key words: flow angle, LES method, suspended pipeline, velocity distribution, vorticity, wake structure

HIGHLIGHT

- The velocity distribution and wake structure characteristics around the suspended section of the pipeline under oblique flows with different angles were numerically and experimentally investigated.

INTRODUCTION

With the expansion of oil and gas pipeline networks in China, underwater pipelines have become an indispensable part of the oil and gas engineering transportation system. Under complex and harsh natural conditions, the crossing pipeline is easily scoured to the suspended state by high-speed water flow. Influenced by the drag force and rising force of flow, the pipeline is prone to yield failure, which seriously threatens the safe operation of the pipeline and the ecological health of the river (Yang *et al.* 2021). The distribution of the flow field and the hydrodynamic characteristics around the suspended section of the pipe are the important factors affecting the force state, and it is also an important reason for the continuous scour of the pipeline (Yang *et al.* 2019).

Due to the rapid change of the flow field around the pipeline, it is difficult to carry out tests. Most scholars tend to use numerical simulation to conduct research, and the related physical experiments are few. By using particle image velocimetry (PIV) and fiber laser Doppler velocimetry (FLDV), Poggi *et al.* (2002), Lin *et al.* (2009) and Hsieh *et al.* (2016) experimentally studied the flow characteristics around the circumference and obtained a relatively accurate flow distribution. Kravchenko & Moin (2000) conducted a numerical study on a pipeline with a Reynolds number of 3,900, the results showed that different calculation methods have great influence on the flow field distribution near the pipeline. Li & Cheng (1999, 2001) simulated the hydrodynamic characteristics around the pipeline under a potential flow model and turbulence model. It was found that the potential flow model could not clearly simulate the wake structure behind the pipeline, so the hydrodynamic characteristics around the pipeline could not be accurately obtained. By contrast, the large eddy simulation (LES) method in the

turbulence model can accurately simulate the generation and shedding of the vortex behind the pipeline, so the turbulent model is the more mainstream calculation model at present. According to the research of Brørs (1999) and Qiao *et al.* (2016), the large eddy simulation method has higher simulation accuracy than the Reynolds average method (RANS) for the flow field around a three-dimensional cylinder, so the LES method is mostly used to solve the turbulence model. In the existing research results, Chen *et al.* (2002), Zhang *et al.* (2011), Chang *et al.* (2016), Xu *et al.* (2018) and Sun *et al.* (2018) simulated the flow field around the submarine pipeline based on a variety of fluid dynamics software such as ANSYS FLUENT, OpenFOAM and FLOW3D. The hydrodynamic characteristics around the pipeline under different velocities, clearance ratios, pipe diameters and other parameters are explored, and the necessity of establishing a three-dimensional numerical model is marked. The research is relatively richly focused, but few scholars have considered the three-dimensional hydrodynamic characteristics near the pipeline under oblique flow. Although Liu *et al.* (2013) had conducted certain research on the flow field around a circular pipeline under oblique flow, the research mainly focused on the turbulence intensity around the pipeline, and the wake state and flow field distribution behind the pipeline need to be further studied.

In actual projects, due to the limitations of topographic conditions, the pipeline cannot always cross the river vertically, and the situation of slanting water scour still exists. This includes submarine pipelines, which are scoured by the ocean current from different directions. Based on this, a three-dimensional flume numerical model was established by using ANSYS Fluent 16.0 software (ANSYS®, Canonsburg, PA, USA) (Canonsburg 2015) and the LES model. By comparison with the physical test data, the true nature of the results of the numerical model is verified, and the three-dimensional characteristics of the flow field around the pipe and the wake structure behind the pipe under the action of oblique flow are investigated. The research results will provide a certain theoretical reference for the analyzing the mechanical characteristics and security operation management of underwater crossing pipelines.

ESTABLISHMENT OF NUMERICAL MODEL

Turbulence model equation and solution method

The turbulence model should be chosen for numerical simulation of high-speed flow scouring suspended pipelines. Although turbulent motion is complex and difficult to describe, the unsteady continuity equation and the Navier–Stokes equation are still applicable to the transient motion, so it is still used as the basic equation to generate a solution. Among the methods to solve the turbulence model, the LES method can not only capture the details of the flow field, but also is better than other methods in the statistics of the cylinder force and the time-average flow field, furthermore, the simulation results are closer to the real flow field. Therefore, the LES model was chosen to solve the turbulence equation. In addition, the Smagorinsky–Lilly model was applied to solve the sub-grid turbulent viscosity coefficient, and the Smagorinsky Constant is $C_s = 1.0$.

Calculation model

The numerical flume calculation model was established according to the hydraulic physical model test. According to the research of Lei *et al.* (1999), the slenderness ratio of the cylinder should not be less than 4, when the flow obliquely acts on the pipeline and the slenderness ratio is greater than 6, the flow field has non-negligible three-dimensional characteristics, so it is very necessary to establish a three-dimensional numerical model. A three-dimensional Cartesian coordinate system with the intersection point of the middle line between the pipe position and the width of the flume as the center of the circle was established in ICEM software. The total length of the computational domain is 0.90 m, including 0.15 m in front of the pipeline, 0.75 m in back of the pipeline, and 0.4 m in width. The height of the computational domain was determined by the test water depth h. The computational domain of the model is shown in Figure 1, and the model computation domain was defined as fluid. In addition, the parameters of the computational domain are shown in Table 1, where d is pipeline diameter, v is average velocity of flow, Re was Reynolds number, θ is flow angle, and e *is* the distance between the pipeline bottom and the flume bottom. The Reynolds number is calculated using the formula $Re = dv\rho/\mu$, where the density of water is $\rho = 998.2$ kg/m^3, and dynamic viscosity is $\mu = 1.003 \times 10^{-3}$ Pa·s.

Mesh division and boundary condition setting

Due to the simple numerical flume model, it requires high computational accuracy to map the accurate wake structure behind the pipeline, the structured grid was selected in ICEM software. For the calculation of the flow field, the grid should be encrypted, and the dimensionless wall distance y^+ was introduced to solve and divide the grid in the near-wall area. The

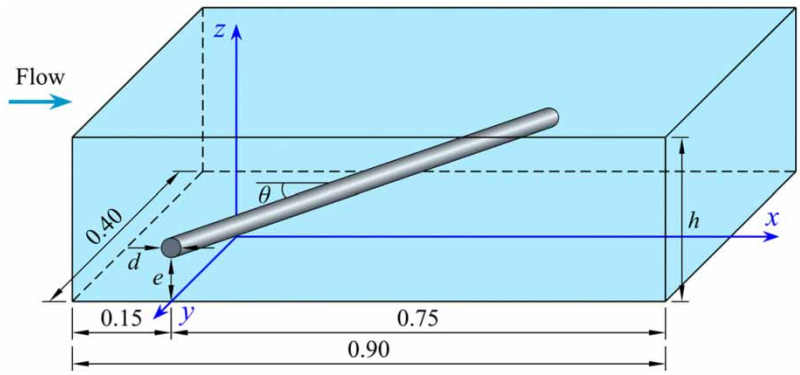

Figure 1 | Schematic diagram of model calculation domain (unit: meter).

Table 1 | Calculation domain parameter table

Pipeline diameter d (m)	Average velocity v (m/s)	Reynolds number Re	Test water depth h (m)	Flow angle θ (°)	Gap ratio e/d
0.03	0.20	5,971	0.244	30	2.00
	0.25	7,464	0.195	45	
	0.30	8,957	0.163	60	
	0.35	10,450	0.139	90	
	0.40	11,943	0.122		

empirical formula is as follows:

$$y^+ = 0.172 \times \left(\frac{\Delta y}{d}\right) \times Re^{0.9} \tag{1}$$

where Δy (m) is the first layer thickness of the grid, d (m) is pipeline diameter, and Re is the Reynolds number.

The O-shaped grid was used to encrypt the 1.5 d range near the pipeline, the number of encryption layers was 2,000 d, and the ratio was 1.05. After many adjustments, the thickness of the first boundary layer near the cylindrical surface was taken as $\Delta y = 0.0025\ d$, and the calculated $y^+ = 0.88 < 1$, meeting the requirements of the solution. The number of grid layers in the span wise direction of the three-dimensional numerical flume model along the width direction of the water tank was 45, and the total number of grids was about 2.5 million. The grid quality was measured by the Determinant $2 \times 2 \times 2$, and the average value of the grid quality parameters was tested. The average grid quality parameter was 0.94, which proved that the grid quality was good. The overall calculation domain grid and near-wall boundary layer grid are shown in Figure 2.

The inlet of the calculation domain selected the flow velocity inlet and set it in sequence according to the average velocity (v) in Table 1. The outlet selected the pressure outlet, and the outlet static pressure was set to 0. Except for the top surface of

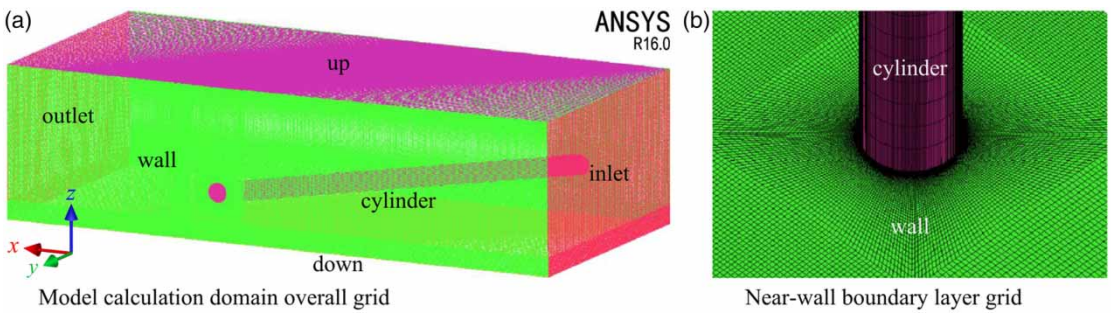

Figure 2 | Schematic diagram of calculation model grid.

Table 2 | Boundary conditions and settings

Types	Boundaries	Settings
Location	Inlet	Velocity inlet
	Outlet	Pressure outlet
	Upper wall (on the top of channel)	Open symmetrical boundary
	Others (under wall, two side walls, cylinder surface)	Non-slip fixed boundary
General	Time	Transient
Viscous model	Model	LES
	Subgrid-scale model	Smagorinsky–Lilly
	Model constants	$C_s = 1.0$
Material	Water liquid	$\rho = 998.2\ \text{kg/m}^3$
		$\mu = 1.003 \times 10^{-3}\ \text{Pa·s}$
Solution method	Pressure–velocity coupling	SIMPLE
Spatial discretization	Gradient	Least squares cell based
	Pressure	Second order
	Momentum	Second order upwind

the flume (up), which was set as an open symmetrical boundary, the other wall surfaces (wall, down, cylinder) were all set to a non-slip fixed boundary. A simple algorithm was used for pressure–velocity coupling of the model, a second-order upwind scheme was chosen for pressure discrete format, and a second-order implicit scheme was used for the transient governing equation. Boundary conditions and settings are shown in Table 2. The normalized time step size is set as 0.005 s to satisfy Courant–Friedrichs–Lewy (CFL) criteria. The number of iteration steps is 6,000, and the total calculated duration is 30 s. After the calculation of the transient model, the time-average flow field model was applied to continue the calculation of 2,000 steps, and the time-average statistics of the flow field within 10 s were performed.

VERIFICATION OF NUMERICAL MODEL

Test data collection

The experiment was carried out in a unidirectional circulating flume with a length of 9.1 m, a width of 0.4 m, and a height of 0.7 m. The schematic diagrams of the flume system and velocity extraction section are shown in Figure 3, in which, the middle

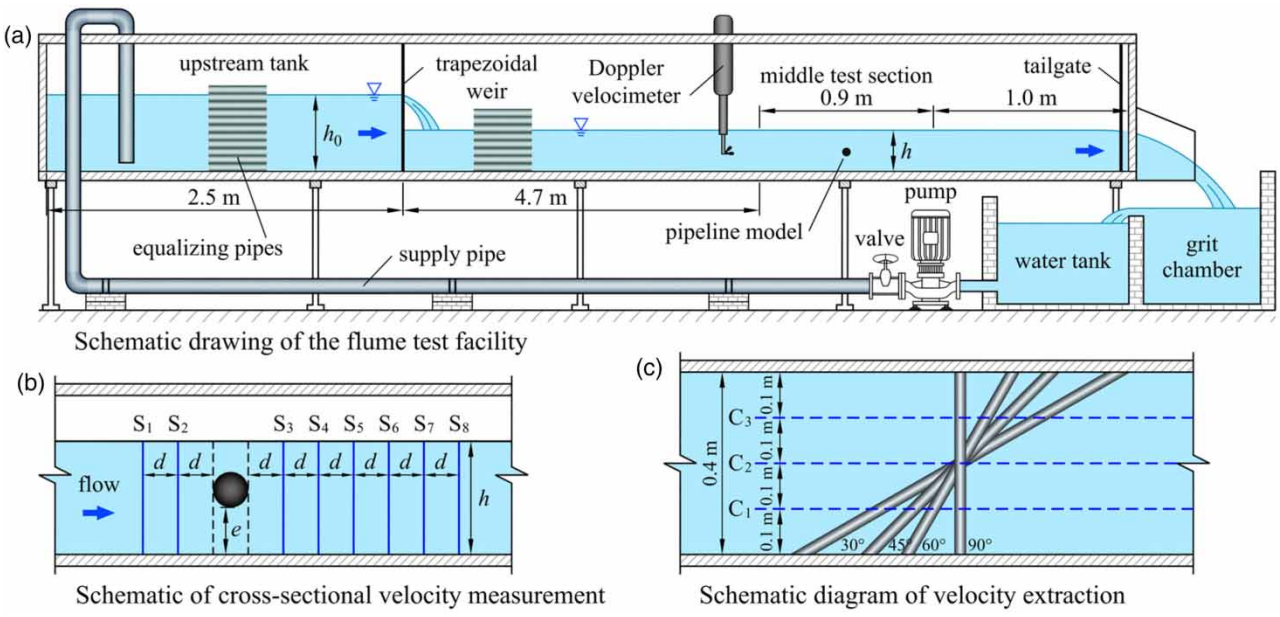

Figure 3 | Experimental setup of the flume model.

test section is 0.9 m long, 4.7 m from the upstream trapezoidal weir, 1.0 m from the downstream tailgate, and the length of the upstream water tank is 2.5 m. The test pipeline is a smooth Plexiglas hollow pipeline with a diameter of 3 cm, ignoring the wall thickness. The distance between the bottom surface of the pipe and the upper surface of the sink is twice the pipe diameter. The water depth of the experiment h is 0.195 m, the average velocity v is 0.25 m/s, and the angle θ is 90°. Water temperature was maintained at 20°C in all tests. A Doppler point current meter was used to collect the velocity along the direction of depth near the pipeline with the midpoint of the width of the flume as the section. The sampling range is 0.01–4.00 m/s, the measurement accuracy is $\pm 0.05\%$ (± 1 mm/s) of the measured value, the sampling frequency is 1–200 Hz, and the sampling distance ≥ 5 cm. The schematic diagram of the collection location is shown in Figure 3(b). At least 10 velocity values along the direction of water depth were collected for each section, and the sampling time was not less than 60 s.

Model validation

The numerical model was calculated under the same working conditions as the experiment, and the average velocity of sections S_1–S_8 at the same time as the experiment was extracted for comparative analysis with the results. The velocity verification results are shown in Figure 4. In addition, using statistical parameters methods, root mean square error between the simulated value and experimental value was 0.0156, and the R-squared (R^2) value to fit the line X = Y was 0.894, where X = simulated value and Y = experimental value. It is obvious that the velocity distribution results calculated by the numerical model at each section are basically consistent with the experimental measurement results, which verifies the reliability of the numerical model. As a consequence, the model can be used for subsequent numerical simulation research on the distribution of three-dimensional flow field.

SIMULATION RESULTS AND ANALYSIS

The influence of the angle on the distribution of velocity near the pipeline

In order to explore the influence of different angles on the three-dimensional flow field and the velocity near the pipe, a section was cut every 0.1 m along the width direction of the flume (y-axis). The schematic diagram of the velocity extraction section is shown in Figure 3(c). For each section C_1, C_2, and C_3, the time-average velocity of section S_1–S_8 near the pipeline along the water depth was extracted respectively. The time-average velocity of 24 sections in three sections was extracted from each group of working conditions. The experimental case of the average velocity $v = 0.40$ m/s was selected as the research object. As shown in Figures 5–8, the velocity distribution of different sections near the pipeline with different flow angles was portrayed in a unified coordinate system.

Through comprehensive analysis of Figures 5–8, it is obvious that, under the action of oblique flow, the velocity distribution near the pipeline presents a relatively three-dimensional characteristic and, the smaller the angle, the more obvious is the characteristic. The amplitude of velocity fluctuation around the pipe increases with the increase of the angle, the smaller the flow angle, how similar the velocity distribution of different sections is along the water depth, and the velocity distribution at different sections changes with the change of the angle between the pipe and the flow. When the angle $\theta = 90°$, the velocity distribution of each section C_1, C_2, and C_3 along the water depth is basically the same. Except for slight differences in the velocity values of a few points near the pipeline, the velocity variation of each section is almost identical. As a result,

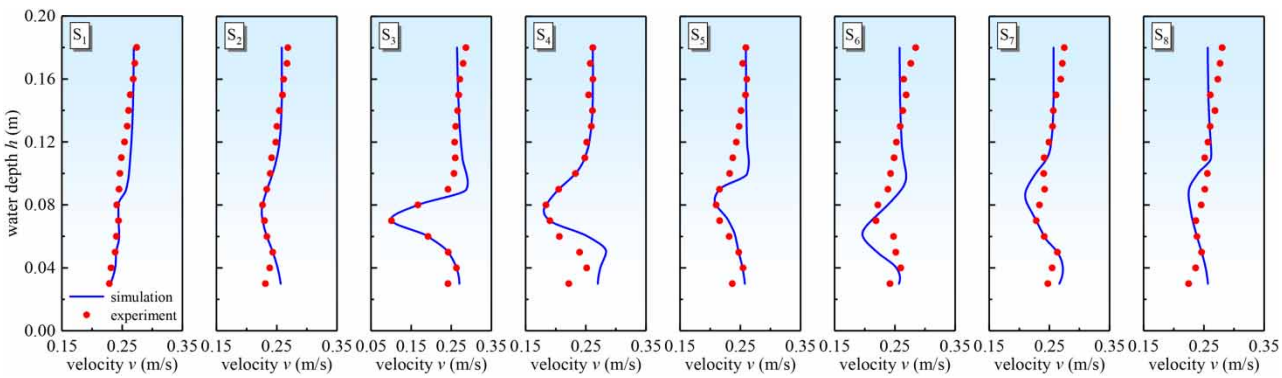

Figure 4 | Verification of flow velocity near the pipeline.

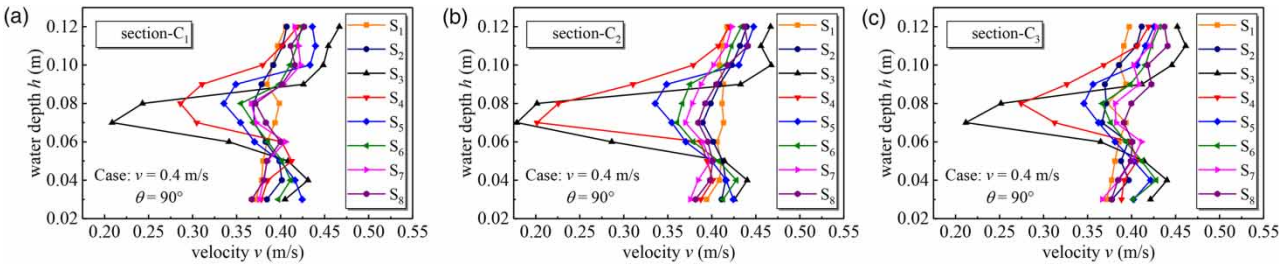

Figure 5 | Velocity distribution of different sections near the pipeline when $\theta = 90°$.

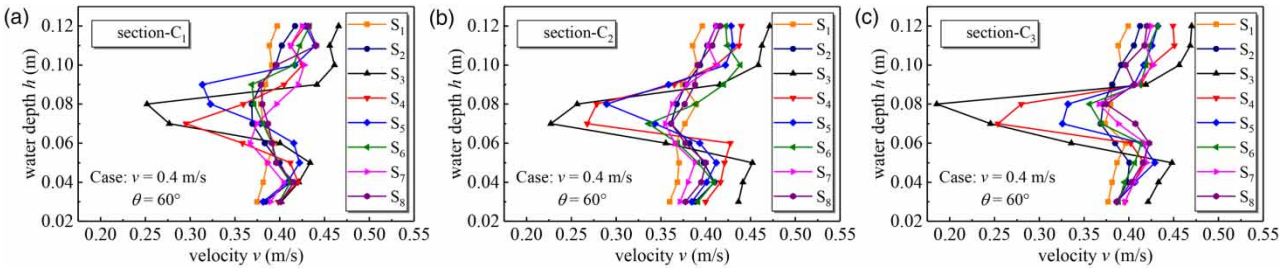

Figure 6 | Velocity distribution of different sections near the pipeline when $\theta = 60°$.

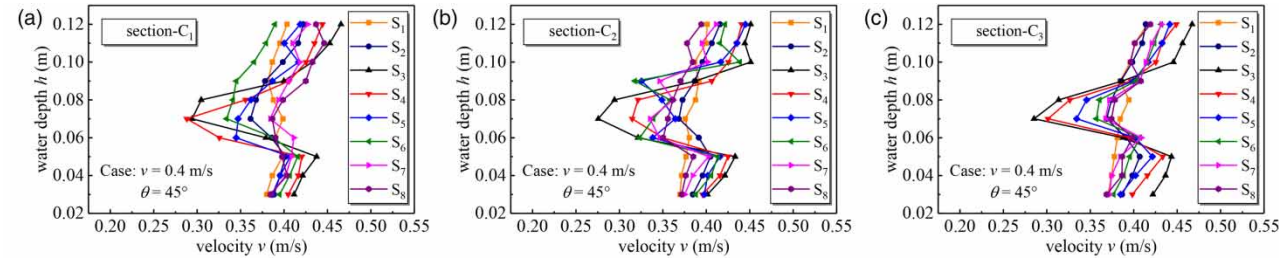

Figure 7 | Velocity distribution of different sections near the pipeline when $\theta = 45°$.

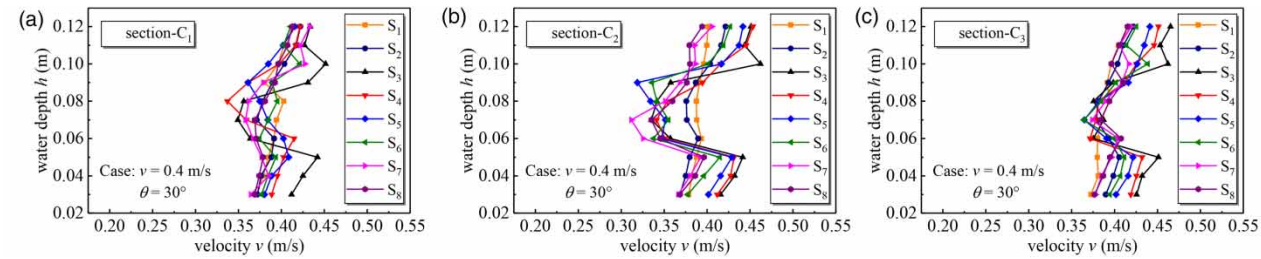

Figure 8 | Velocity distribution of different sections near the pipeline when $\theta = 30°$.

when the flow is perpendicular to the pipeline, it can be concluded that the velocity distribution near the pipeline does not have a three-dimensional effect, and it is sufficient to analyze the two-dimensional results.

With the decrease of the angle between the pipe and flow, the velocity distribution near the pipe gradually shows more and more obvious three-dimensional effects. At the same time, the velocity distribution gap of each section of the pipeline is also increasing, the variation amplitude changes, and the velocity distribution law is gradually weakened. When the angle $\theta = 60°$, the maximum fluctuation amplitude of velocity on sections C_1–C_3 increases in turn, and reaches the maximum at section C_3. When angle $\theta = 45°$ and 30°, the maximum velocity fluctuation amplitude at section C_2 reaches the peak, and the velocity fluctuation amplitude has gradually become disorderly. The velocity distribution becomes obviously disordered and loses

its original rule when the angle is 30°. The primary reason for this phenomenon is that the wake structure behind the pipe gradually presents an increasingly obvious three-dimensional effect with the different angles. That is, the smaller the angle, and the more irregular the vortex shedding characteristics of the pipeline, the more disorderly is the velocity distribution.

In order to study the relationship between the velocity distribution along water depth and the angle of flow at different sections, the velocities of different sections at the middle section C_2 of the flume under this working condition were taken for detailed analysis, as shown in Figure 9.

By comparing the velocity distribution of the eight sections, it is not difficult to find that the velocity distributions along the water depths of S_1 and S_2 within the range of twice pipe diameter in front of the pipe is less affected by the pipe. The velocity distribution of S_1 is almost unaffected by the existence of the pipeline, that is, the velocity decreases gradually with the depth of the water. The velocity distribution of S_2 is affected by the existence of the pipeline, and there is a slight S-shaped change tendency near the pipeline, but the overall velocity is still gradually decreasing along the water depth. The flow velocity of S_3 in the range of once pipe diameter behind the pipe is most affected by the pipeline, the velocity distribution curve here shows an obvious 'S' shape, and the velocity above the pipe still presents a parabolic distribution along the water depth. However, due to the rapid turbulence of the water near the pipeline, the velocity changes greatly, where the velocity deficit reaches the maximum here, which can exceed 0.5 v. After the sudden change of the velocity, there will be an abnormally increased velocity value at 0.5 d below the pipeline, which is usually called the velocity reversal value. The velocity at this point can be greater than the average velocity of the section, which is also called the near-bottom velocity of the pipeline. Therefore, it can be considered that the abnormal increase of the velocity value is an important reason for local scour of the pipeline. Then the velocity continues to decrease along the water depth according to the law of gradient decline. With the increase in the distance with the pipeline, the influence of the pipeline on the velocity distribution of S_4–S_8 behind the pipeline is gradually weakened. The shape of 'S' is less and less obvious, and it can be inferred that S_8 is almost not affected by the presence of pipeline. As a result, it can be preliminarily judged that the influence range of the pipeline on the velocity is within the range of one times diameter before and six times diameter behind the pipe.

Through comparing the velocity distribution of each section under different angles, it can be deduced that with the increase of the angle between pipe and flow, the velocity changes more dramatically. It is most obvious at S_3 and S_4, and the greater the angle, the more 'sharp' the bulge and the more obvious the change. The main reason for this variation is that the velocity behind the pipeline is greatest when the pipeline vertically crossing the water flow. However, for the oblique flows, the component of flow velocity along the axial direction of the pipeline causes a decrease in the velocity along the flow direction. The smaller the angle, the smaller the velocity in the direction of water flow, and the weaker the velocity changed. The velocity distribution of S_5–S_8 behind the pipeline does not change with the angle changed, and it does not change the most when the angle is 90°. When $\theta = 60°$ at S_5, the loss of flow velocity reaches the largest, and when $\theta = 45°$ at S_6, the loss of flow velocity is the largest. The loss of velocity is the largest when $\theta = 30°$ at S_7 and S_8. Since the velocity distribution behind the pipe is gradually weakened by the influence of the pipe and the regularity of the flow around the pipe is poor, the above phenomena are highly likely to occur. It is worth noting that in sections S_5–S_8, when the oblique flow occurs, the velocity near the pipe will appear to undergo a 'zigzag' change, the increase and decrease of the velocity occur alternately. The reason for this

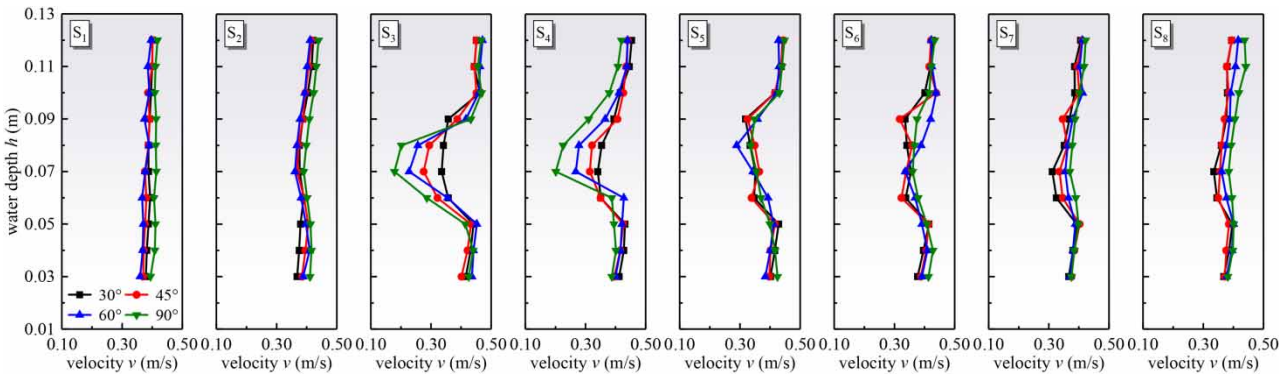

Figure 9 | Velocity distribution of cross-section C_2 with different flow angles.

phenomenon may be that the pattern of vortex shedding in the back of the pipeline becomes less regular with the decrease of the angle, and the irregular vortex shedding is likely to lead to the alternation of the flow velocity behind the pipeline.

Influence of the angle on wake flow structure behind pipeline

We took the working condition of velocity $v = 0.20$ m/s to compare and analyze the wake structure behind the pipeline at different flow angles. In order to verify whether the wake structure under different pipe flow angles has three-dimensional characteristics, the wake flow characteristics behind the pipeline at C_1, C_2, and C_3 are shown successively. The vertical view of the structural characteristics of the rear wake of the pipeline at the dimensionless time of $(v{\cdot}t)/d = 200$ with different angles are shown in Figure 10.

It can be seen from the figure that, when the pipeline is perpendicular to the flow direction, the characteristics of vortex shedding at the three sections of the pipe are basically the same, and the three-dimensional effect is not significant. When the water flow acts on the pipeline diagonally, the vortex street behind the pipeline can still be shed regularly, but the shape of the vortex street is disorderly, and the vorticity value varies greatly, accompanied by many small vortex streets. With the decrease in the angle, the shape of the vortex street behind the tube becomes more and more unclear. When the angle is 30°, it is almost impossible to identify the regular Karman vortex street accurately. The vortex shedding behind the pipe at different sections is also quite different. The number of vortex streets at C_1 is significantly more than that at C_2 and C_3. The closer to the back wall of the tank, the clearer the shape of vortex streets, the more obvious the shedding rule, and the longer the length of the wake area. In addition, the three-dimensional characteristics of the wake structure behind the pipeline become more and more significant with the decrease of the angle. At the same velocity, the length of the backflow area and wake area behind the pipe decreases with the decrease of the angle, the distance of the first vortex street behind the pipe increases with the decrease of the angle, and the number of vortex shedding decreases with the decrease of the angle. When the angle is 90°, it can reach seven, and when the angle is 30°, there are only one or two clearly identifiable whirlpools behind the pipe. It can be inferred that the vortex shedding frequency behind the pipeline is greatly affected by the angle between pipe and flow, and the smaller the angle, the lower will be the vortex shedding frequency.

In order to further study the wake morphology behind the pipeline at different sections under the action of oblique flow, the wake morphology of different sections at the angle $\theta = 60°$, 45°, and 30° was ploted in TECPLOT software, as shown in Figure 11. The vorticity unit and scale in the figure are the same as those in Figure 10.

By comparing the wake structure diagram behind the pipeline at different angles at the same section, it can be concluded that the thickness of the boundary layer near the pipeline decreases with the decrease of the angle. The length of the backflow area behind the tube, the vorticity in the backflow area, and the number of regular Karman vortex streets behind the pipeline

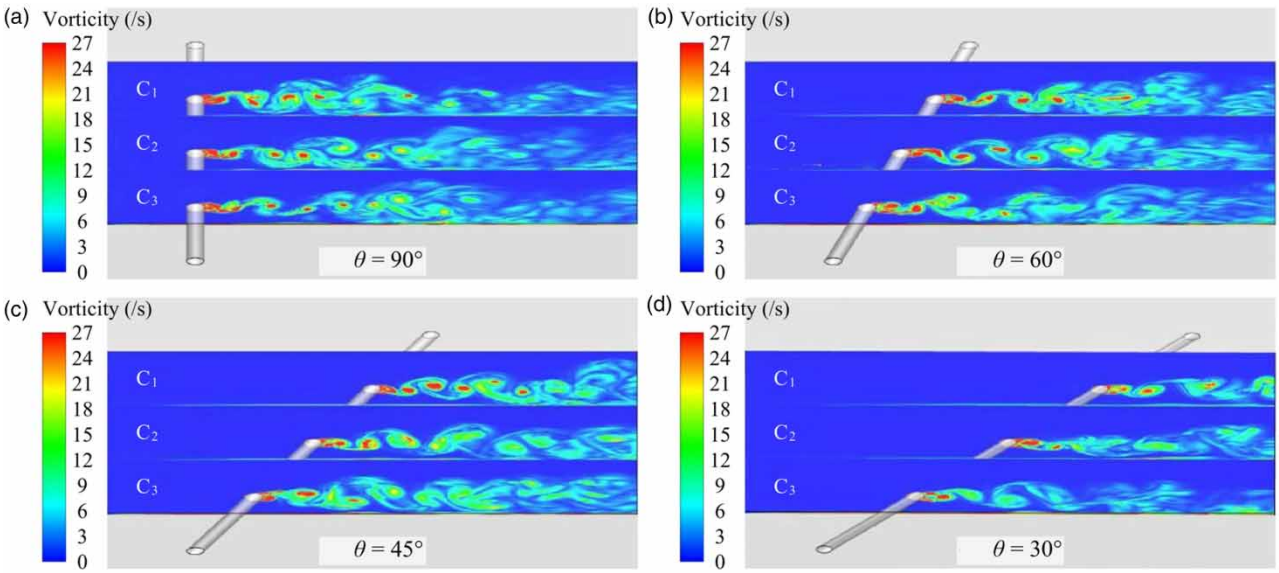

Figure 10 | Wake structure behind the pipeline under different flow angles.

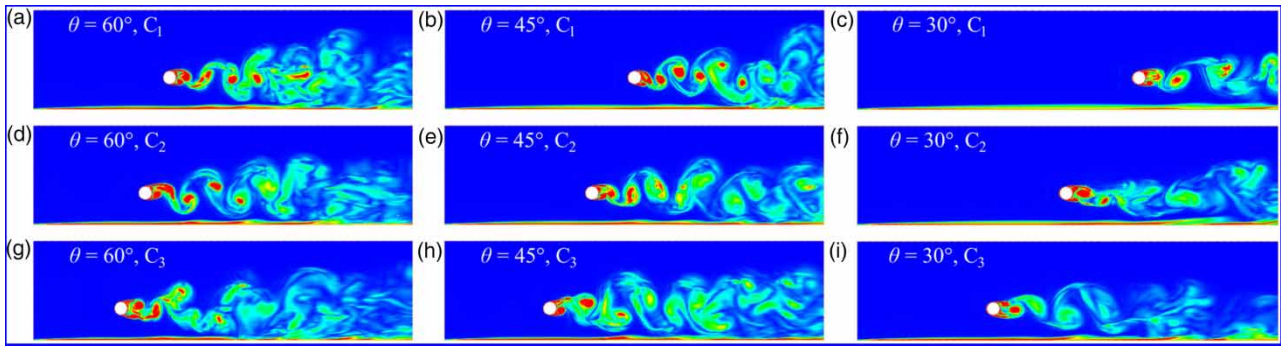

Figure 11 | Wake structure diagram of different cross-sections of pipeline under oblique water flow.

decreases accordingly. By contrast, the distance between two adjacent vortex streets increases with the decrease of the angle. With the decrease of the angle, the length and width of the wake area behind the pipe at each section also decrease significantly. It can be seen that there is a certain phase difference in the frequency of vortex shedding between sections through comparing the characteristics of vortex shedding behind pipes with different sections at the same angle. According to the law of flow, the water that reaches the vicinity of the pipeline separates first, generating vortex streets of a certain size and number, followed by those that arrive later. At the same time, the number of vortex streets arriving at the section near the pipe first is large and the shape of vortex streets is clear, while the number of vortex streets arriving later is less and the shape of vortex streets is chaotic, which is also an important reason for the three-dimensional characteristics of the wake structure behind the pipe. When the water flows obliquely on the pipeline, there is a certain component of the flow along the axial direction of the pipeline, the smaller the angle, the larger is the component. The existence of the axial component hinders the falling off of the vortex behind the pipe, making it more difficult to form the Karman vortex street behind the pipe, which is more obvious from Figure 11(c), 11(f) and 11(i). When the angle is 30°, the shape of the vortex street behind the tube is almost indistinguishable. Therefore, it can be concluded that the flow field behind the inclined pipe must be disturbed.

In order to analyze the wake structure behind the pipeline more intuitively, the calculation results were imported into CFD-POST to establish the core area of vorticity by using the *Q*-Criterion (Hunt *et al.* 1988) to define the three-dimensional vorticity equipotential surface, using the speed variable to color. Since the velocity is small, the value $Q = 10$ is set, and the three-dimensional vorticity diagram behind the pipeline at angles is shown in Figure 12.

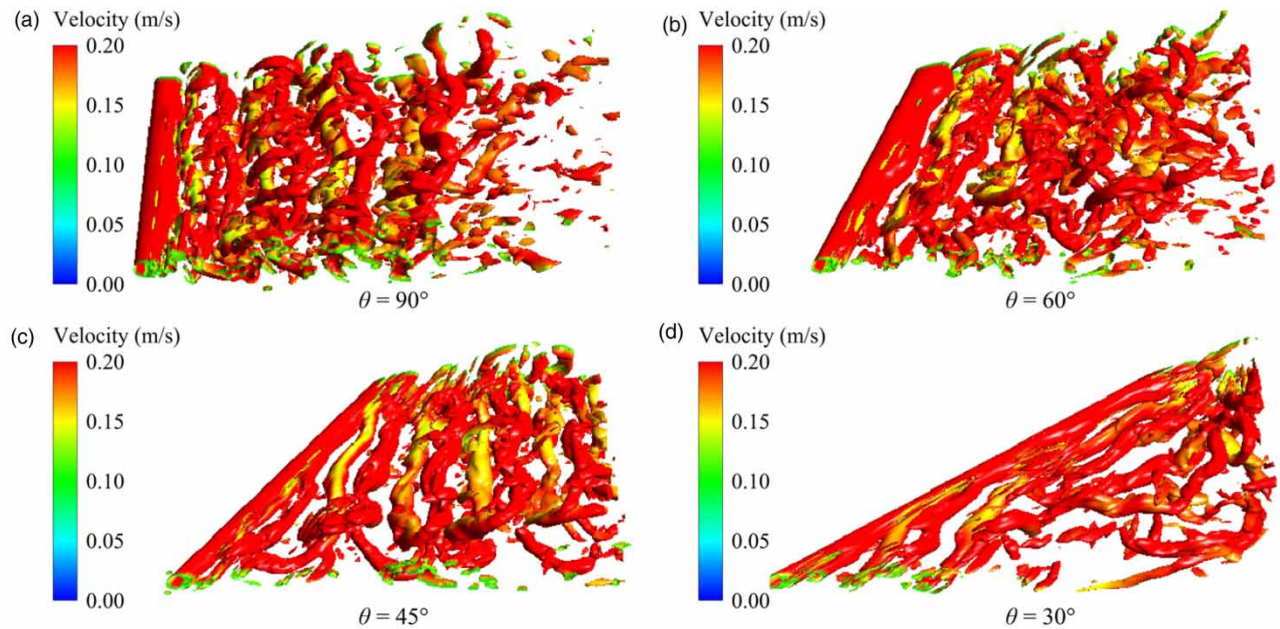

Figure 12 | Three-dimensional vorticity equipotential surface of wake under different flow angles.

Under the same vorticity value, with the decrease of the angle, the number of vortex streets behind the tube decreases significantly and becomes more and more irregular. When $\theta = 30°$, the three-dimensional vortex street behind the pipe has become very rare and irregular, the shape of the vortex street has been completely destroyed, and the water turbulence behind the pipe is turbulent. In addition, with the decrease of the angle, the vortex shedding angle increases obviously, and the shedding degree becomes looser, and the closer to the front wall of the tank, the more obvious it is. It is also verified that the axial flow component of the pipe has a great influence on the frequency, quantity, angle and shape of the vortex shedding of the pipe.

Under the oblique flow, the three-dimensional structure change of the wake behind the pipeline with the change of velocity is shown in Figure 13. The vorticity value Q is 5 when the velocity is $v = 0.20$ m/s, 10 when $v = 0.30$ m/s, and 15 when $v = 0.40$ m/s. By comparing the change of the wake structure of the pipe with the velocity under different angles, it is concluded that the larger the angle, the more dramatic the change of the wake structure behind the pipe with the velocity, the more the length of the corresponding backflow area and wake area grows, the larger the proportion of the growth of the number of vortex falling off, and the more regular the change. With the decrease of the angle, the regularity of the change of the wake decreases. When the angle is 30°, the structure of the wake area changes little with the velocity, and the characteristics of the vortex shedding are less affected by the velocity. In other words, the regularity of vortex shedding has been lost.

CONCLUSIONS

The three-dimensional numerical model of flume was established using ANSYS Fluent software in the LES method. On the basis of verifying the reliability of the model through the measurement results of the physical model test, the influence of the angle on the velocity distribution and wake structure behind the pipeline was explored, and the following conclusions were obtained.

(1) When the water flow acts vertically on the pipeline, the velocity distribution near the pipeline does not have a three-dimensional effect. With the decrease in the angle, the three-dimensional characteristics of the velocity distribution around the pipeline are gradually enhanced. The section position of the peak velocity fluctuation changes in a disorderly way with the change of the angle, and the velocity distribution becomes more turbulent.

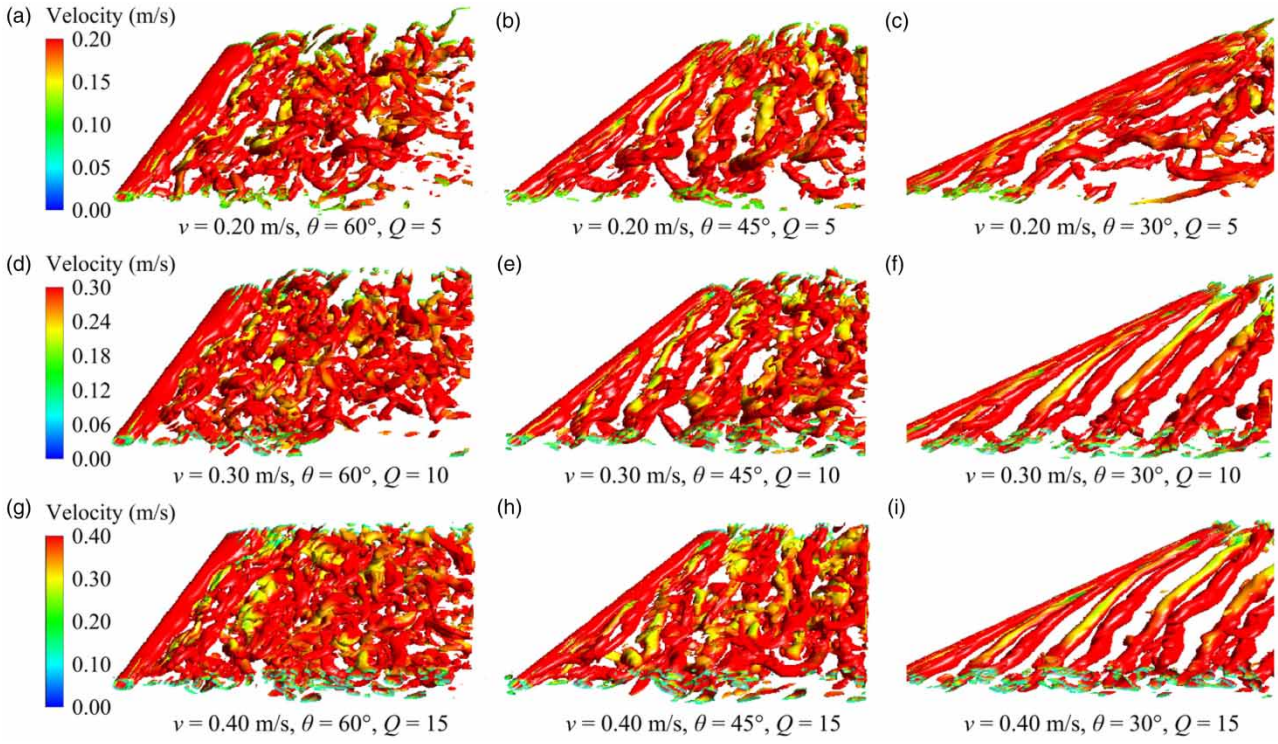

Figure 13 | Variation of vorticity equipotential surface with velocity under different pipe flow angles.

(2) The influence range of pipeline on velocity is 1 d before and 6 d behind the pipeline. The velocity change of section which is 1 d behind the pipe is most affected by the pipeline, and the velocity distribution shows an obvious 'S' shape, where the velocity deficit near the pipeline reaches the maximum, exceeding 0.5 v. The abnormally increasing velocity reversal value at 0.5 d below the pipeline is also an important reason for local scour of the pipeline.

(3) The three-dimensional effect of the wake structure behind the pipe increases gradually with the decrease of the angle. When the angle is 90°, it can be considered that there is no three-dimensional effect. With the decrease of the angle, the different vortex shedding patterns of pipes at different sections are greater, and the vortex shedding frequencies at different sections have certain phase differences. The closer to the back wall of the flume, the clearer the vortex structure, and the more the number of vortex sheddings.

(4) The thickness of the boundary layer near the pipeline, the backflow area behind the pipeline, the length of the wake area and the vortex shedding frequency all decrease with the decrease in the included angle of the pipe flow, and the distance between adjacent vortex streets also decreases significantly. Under the oblique flow direction, there is a certain flow component in the axis direction of the pipe, which is the main reason for the three-dimensional flow field disorder behind the pipe, and the smaller the angle, the more disordered is the flow field.

(5) The Q-Criterion is used to define the three-dimensional vorticity equipotential surface to describe the three-dimensional flow field behind the pipeline, which can more intuitively reflect the distribution rule of flow field. The larger the angle, the more dramatic is the change in the wake structure behind the pipe with the velocity, and the more obvious is the change regularity. With the decrease of the angle, the structure of the wake behind the tube becomes weaker with the velocity, and the vortex shedding gradually loses regularity.

ACKNOWLEDGEMENTS

This work was supported by the National Natural Science Foundation of China (Grant No. 51478403).

DATA AVAILABILITY STATEMENT

All relevant data are included in the paper or its Supplementary Information.

REFERENCES

ANSYS Fluent Theory Guide; Release 16.0 2015. ANSYS Inc., Canonsburg, PA, USA.

Brørs, B. 1999 Numerical modeling of flow and scour at pipelines. *Journal of Hydraulic Engineering* **125** (5), 511–523.

Chang, L., Jiang, C. & Cheng, Y. 2016 Experimental study on the hydrodynamics around marine pipelines under oblique flows. *Periodical of Ocean University of China* **46** (7), 105–110.

Chen, B., Li, Y. & Lai, G. 2002 Three-dimensional calculation of oscillating flow past a circular cylinder near a plane. *Chinese Journal of Hydrodynamics* **17** (1), 9–16.

Hsieh, S., Low, Y. & Chiew, Y. 2016 Flow characteristics around a circular cylinder subjected to vortex-induced vibration near a plane boundary. *Journal of Fluids and Structures* **65**, 257–277.

Hunt, J., Wray, A. A. & Moin, P. 1988 Eddies, streams, and convergence zones in turbulent flows. In: *Center for Turbulence Research Proceedings of the Summer Program 1988*. pp. 193–208.

Kravchenko, A. G. & Moin, P. 2000 Numerical studies of flow over a circular cylinder at $Re_D = 3900$. *Physics of Fluids* **12** (2), 403–417.

Lei, C., Cheng, L. & Kavanagh, K. 1999 Re-examination of the effect of a plane boundary on force and vortex shedding of a circular cylinder. *Journal of Wind Engineering & Industrial Aerodynamics* **80** (3), 263–286.

Li, F. & Cheng, L. 1999 Numerical model for local scour under offshore pipelines. *Journal of Hydraulic Engineering* **125** (4), 400–406.

Li, F. & Cheng, L. 2001 Prediction of lee-wake scouring of pipelines in currents. *Journal of Waterway, Port, Coastal, and Ocean Engineering* **127** (2), 106–112.

Lin, W., Lin, C., Hsieh, S. & Dey, S. 2009 Flow characteristics around a circular cylinder placed horizontally above a plane boundary. *Journal of Engineering Mechanics* **135** (7), 697–716.

Liu, B., Cheng, Y., Liu, C. & Wang, J. 2013 Mathematical simulation and experimental research on the flow around submarine pipelines under the oblique flow. In: *Proceedings of the 16th China Ocean (Shore) Engineering Symposium*. pp. 429–434.

Poggi, D., Porporato, A. & Ridolfi, L. 2002 An experimental contribution to near-wall measurements by means of a special laser Doppler anemometry technique. *Experiments in Fluids* **32** (3), 366–375.

Qiao, Y., Gui, H. & Liu, X. 2016 Analysis of three-dimensional numerical simulation methods for turbulent flow past circular cylinder. *Hydro-Science and Engineering* **3**, 119–125.

Sun, Z., Zhang, D., Liu, L. & Bai, Y. 2018 Analysis of flow around a near wall cylinder of submarine pipeline suspended span. *Ship Engineering* **40** (6), 106–111.

Xu, M., Chen, X., Wang, B., Guan, W., Fan, Z. & Dong, J. 2018 Large eddy numerical simulation of flow characteristics around submarine pipeline. *Fluid Machinery* **46** (5), 18–24.

Yang, Q., Sun, M., He, M. & Yang, Q. 2019 Experimental study on evolution properties of riverbed near underwater crossing pipeline. *Natural Gas Industry* **39** (10), 110–117.

Yang, Q., Zhang, Y., Yang, Q. & Wang, Z. 2021 Experimental study on the loading capacity of suspended section of underwater crossing pipeline. *Advanced Engineering Sciences* **53** (2), 19–27.

Zhang, Z., Shi, B., Ruan, X. & Gao, X. 2011 Two-dimensional numerical simulation and experimental study of flow around submarine pipeline at various gap-ratios. *Periodical of Ocean University of China* **41** (9), 90–94, 108.

First received 2 August 2021; accepted in revised form 4 February 2022. Available online 17 February 2022